Impact assessment of multiple uncertainty sources on high flows under climate change

Ye Tian, Yue-Ping Xu, Martijn J. Booij and Long Cao

ABSTRACT

This paper aims to investigate the uncertainty ranges of high flows under climate change in Jinhua River basin, eastern China. Four representative concentration pathways (RCPs), three global climate models (GCMs), 10 downscaling parameter sets and three hydrologic models are applied to simulate future discharges. Changes of annual maximum discharges are assessed for the baseline period (1961–1990) and future period (2011–2040). The uncertainties of annual maximum discharges are calculated for each uncertainty source and compared with different combinations of them. The minimum temperature will probably increase all year round in the future period and maximum temperature would increase in most cases. The changes of precipitation showed different directions by different models and emission scenarios. The annual maximum discharges would decrease for all RCPs. The order of uncertainty ranges of high flows due to different uncertainty sources from high to low is: hydrologic models, GCMs, parameter sets in the downscaling method and emission scenarios. It must be noted that the small uncertainty contribution from different emission scenarios is due to the study period when the differences in increase of radiative forcing and greenhouse gas concentration are less obvious between different RCPs compared to the second half of the 21st century.

Key words | climate change, eastern China, extreme high flows, uncertainties

Ye Tian
Yue-Ping Xu (corresponding author)
Department of Civil Engineering,
Institute of Hydrology and Water Resources,
Zhejiang University,
Hangzhou,
Zhejiang,
China
E-mail: *yuepingxu@zju.edu.cn*

Martijn J. Booij
Department of Water Engineering and Management,
Faculty of Engineering Technology,
University of Twente,
Enschede,
The Netherlands

Ye Tian
Long Cao
Department of Earth Science,
Zhejiang University,
Hangzhou,
Zhejiang,
China

INTRODUCTION

Extreme hydrological events like floods are one of the most severe natural disasters which have caused great economic losses and casualties in many places in the world (Kundzewicz *et al.* 2010; Sena *et al.* 2012a). Floods are closely related to the climate system and are usually very localized and sensitive to even modest changes of climate equivalent or smaller than changes expected from potential global warming (Knox 2000). Previous studies show that the frequency and intensity of the extreme climatic and hydrological events have been increasing and are likely to continue to increase due to global warming (Easterling *et al.* 2000; Bell *et al.* 2004). In China, over the past 40 years about 50% of summer precipitation in the lower and middle Yangtze River is in the form of rainstorms which brings an increasing risk of summer flood (Jiang *et al.* 2007). Similarly, in the Pearl River basin extreme flood events have significantly increased since 1980 (Wu *et al.* 2013). In coastal regions like Zhejiang Province, where the study basin is located, climate change has exerted impacts on the hydrologic cycle and affected river runoff. Typhoons usually bring much precipitation and cause floods almost every year, and there has been a significant increasing tendency in the past five decades (Tian *et al.* 2012; Xu *et al.* 2012, 2013).

Many studies on the impact of climate change on regional water resources focused on the long term average flows, but it is acknowledged that climate change may severely affect extreme events in hydrology on a regional scale (Sena *et al.* 2012b; Zakaria *et al.* 2012). Extreme events are of most concern for water management and hazard prevention (Qi *et al.* 2013). However, the ability to predict extreme events is much less compared to average

doi: 10.2166/nh.2015.008

flow events (Hirsch 2011; Tian *et al.* 2013). There is less confidence about changes in extremes than that in average flows (Alliance 2009; Tian *et al.* 2014). Besides, the uncertainty of future extreme events may increase with future climate variability and change, which requires us to develop a broader understanding of the range of possible hydrologic futures that we may face (Rolf *et al.* 2010).

In impact studies of climate change on hydrology, commonly there are four steps involved (Horton *et al.* 2006; Wilby & Harris 2006; Camici *et al.* 2014). First, the scenarios are set up to assist in understanding the possible future developments of the climate. Secondly, the global climate models (GCMs) are applied to project the future climate under different climate scenarios. Then, because of the mismatch between the resolution of GCMs and hydrologic models, downscaling of GCM projections is implemented to refine the GCM data so that the resolution could be compatible with the hydrologic models. Lastly, the downscaled GCM outputs are used as input to drive the hydrologic models to simulate for instance river discharge at regional or local scales.

However, the impact assessment of future climate change is subject to a series of uncertainties. Owing to limited knowledge of the reality and unpredictable future, uncertainties are inevitable in every step of the modeling process. There are many different classifications of uncertainty sources for various research purposes (Van der Keur *et al.* 2008; Warmink *et al.* 2011). In terms of the location, level and nature of uncertainties, Walker *et al.* (2003) defined several uncertainties that should be taken into account in uncertainty analysis, including model context, input, model structure and parameters. Xu *et al.* (2005) discussed the challenges and problems in studying hydrological consequences of climate change and pointed out that there are large uncertainties in climate scenarios, GCM output, downscaling methods and hydrologic models. Previous studies have analyzed the uncertainty from GCMs, scenarios, hydrological model input and hydrological models (Wilby & Harris 2006; Chen *et al.* 2013b), however, only limited studies on the uncertainty of downscaling methods compared to other uncertainty sources could be found. In this study, we did not aim to investigate the uncertainty caused by different downscaling methods. This has been done by several studies (Wilby *et al.* 1998; Chen *et al.* 2013a; Tofiq & Guven 2014). This study focused on the uncertainty of a statistical downscaling method, and made a comparative analysis to other uncertainty sources including GCMs, scenarios and hydrological models. The assessment of uncertainty along the whole modeling process is crucial because it provides more informative projections of climate change impacts on the river discharge and it is fundamental to improve the existing modeling techniques. Besides, it provides scientific support for policymakers in water resources management to make a robust decision under climate change.

Climate scenarios are possible images of the future. They are developed to describe how the future might be with respect to socio-economy, technology and emission of greenhouse gases. In the 1992 Supplementary Report to the IPCC Assessment, six alternative IPCC scenarios (IS92) were published which embodied a series of assumptions that have impacts on future greenhouse gas emissions without considering climate policies (Houghton *et al.* 1992). Based on IS92, in 2000 a set of IPCC scenarios which estimated the uncertainty of greenhouse gas emissions was published in the Special Report on Emission Scenarios (SRES) (Nakicenovic *et al.* 2000). Similarly as IS92, the SRES scenarios assumed no policy actions in climate change mitigation and adaptation either. Recently, the SRES scenarios were updated and expanded for the purposes that firstly more detailed information is needed in running the current generation of climate models, and secondly there is an increasing interest in exploring the impact of different climate policies (Van Vuuren *et al.* 2011a). The newly developed scenarios are called representative concentration pathways (RCPs), which have provided a new basis for climate modeling. Up to now, there have been some studies on the assessment of simulation results for the different RCPs from the ensemble of Coupled Model Intercomparison Phase Five (CMIP5), and comparison between CMIP5 and CMIP3 (Moss *et al.* 2010; Knutti & Sedláček 2012). However, only few studies on extreme hydrology including quantification of all uncertainty sources under the new RCPs have been carried out.

This study investigates the uncertainties in extreme flows originating from RCPs, GCMs, downscaling method and hydrologic models. The major objective is to assess the impact of climate change on extreme discharges and

to quantify the uncertainty of extreme flows stemming from different sources. The paper is organized as follows. First, the study area and the observed data are presented in the following section. Subsequently, the scenarios, GCMs, downscaling method and hydrologic models applied in this study are described. Then, the results are presented followed by the discussion section. Conclusions are drawn are in the final section.

STUDY AREA AND DATA

Jinhua River has a drainage area of approximately 6,000 km^2. The Jinhua River basin is a subbasin of Qiantang River basin which is the largest and most important water resource for Zhejiang Province in eastern China. Two major tributaries, Dongyang River and Wuyi River, form the Jinhua River. The Jinhua River basin has a typical subtropical monsoon climate with large inter-seasonal variability in temperature and precipitation. The annual mean precipitation from 1953 to 2008 was 1,386 mm. The annual maximum discharge at Jinhua station varied between 600 and 4,900 m^3/s in the period 1961–1990. Almost every year floods occur in summer when typhoons bring much precipitation, and floods often cause great property loss and casualties (Tian *et al.* 2012).

In this study, observed daily discharge and climate data from 1981 to 1995 are used to calibrate (1981–1990) and validate (1991–1995) the hydrologic models (Table 1). For the comparison of changes between historical and future extreme discharges, monthly climate data in Jinhua River basin from three GCMs, namely BCC-CSM1.1, HadGEM2-ES and GISS-E2-R, for the period 1961–1990 and 2011–2040 are used as baseline and future climate data to drive the hydrologic models. The observed daily climate data from 1961 to 1990 are used for the downscaling method. The discharge station is located at the mouth of the river basin and the weather stations are distributed in the river basin, as shown in Figure 1.

Table 1 | Information of hydrological and climate data

	Stations	Latitude (°N)	Longitude (°E)	Period
Discharge				
	Jinhua	29.08	119.62	1961–1995
Temperature and precipitation				
	Jinhua	29.08	119.62	1961–1995
	Bada	29.20	120.50	1981–1995
	Yiwu	29.30	120.07	1981–1995
	Yongkang	28.90	120.02	1981–1995
	Zhengzhai	28.90	119.63	1981–1995

METHODS

RCPs

The latest emission scenarios called Representative Concentration Pathways were developed to update and expand the scope of the old scenarios (Moss *et al.* 2010; Van Vuuren

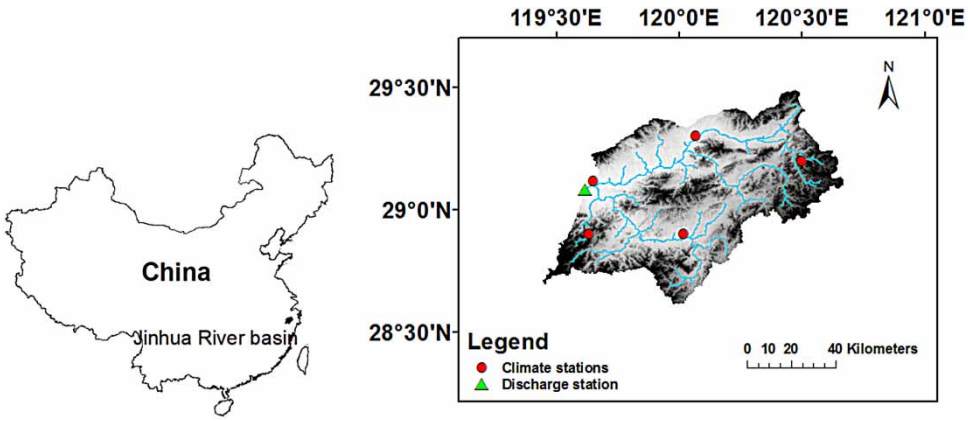

Figure 1 | Location of the Jinhua River basin and distribution of weather and discharge stations.

et al. 2011b). The four RCPs (RCP2.6, RCP4.5, RCP6.0 and RCP8.5) contain information on emissions, concentrations and radioactive forcing, which are used as input for climate model experiments. RCP2.6 represents a mitigation scenario leading to a low forcing level. RCP4.5 and RCP6.5 represent two medium stabilization scenarios. RCP 8.5 represents a high baseline emission scenario (Van Vuuren et al. 2011a). These four RCPs cover the full range of radioactive forcing values from 2.6 to 8.5 W/m^2 and greenhouse gas emissions in the literature.

GCMs

The general circulation model is widely used to simulate climate changes as input for impact assessment studies (Shackley et al. 1998; Murphy et al. 2004; Lobell et al. 2008). In this study, the GCM outputs are derived from a multi-model data set of the World Climate Research Programme's Coupled CMIP5. CMIP5 has been carried out by a broad climate research community and aimed to provide a multi-model context for the assessment of the uncertainties of emission scenarios, model structures and initial conditions. It involves simulations from more than 20 modeling groups using more than 50 models. To make a comparison and analyze the uncertainties of different GCMs, three GCMs are selected. These three GCMs are different in many ways like grids division, boundary conditions and atmospheric compositions. The information of the three GCMs BCC-CSM 1.1 (Wu et al. 2008; Wu 2012), HadGEM2-ES (Jones et al. 2011) and GISS-E2-R applied in this study is given in Table 2.

Downscaling method

LARS-WG is a stochastic weather generator which is commonly used for generating long time series of weather data and producing local daily climate change scenarios for a single site (Lazzarotto et al. 2010; Xu et al. 2012; Calanca & Semenov 2013). It has been tested by many researchers and shows generally a good performance in representing extreme events (Qian et al. 2008; Semenov 2008; Roshan et al. 2013).

Firstly, the statistical features of the observed weather data (in this study daily precipitation, maximum temperature and minimum temperature) are determined. Secondly, the monthly changes in equivalent variables from combinations of the four RCPs and three GCMs were calculated. At last, the synthetic weather data with the same statistical characteristics are generated on a day-to-day basis. The simulation of precipitation occurrence in LARS-WG utilizes a semi-empirical distribution for the length of wet and dry day series and daily precipitation. For a wet day, the value of the precipitation is generated from a semi-empirical distribution of precipitation for the particular month independent of the length of the wet series and the amount of precipitation on a previous day. Daily maximum and minimum temperature are regarded as stochastic processes with daily means and standard deviation conditioned on the wet or dry days (Semenov & Barrow 2002).

Ten sets of 30-year daily meteorological series are produced by varying random seeds which are predefined in LARS-WG. Random seeds control the stochastic component of LARS-WG and make it possible to generate a number of various realizations of the weather time series. These series are used as the input for the hydrological models to study the uncertainty of the downscaling method.

Table 2 | Information about the GCMs in this study

Country	Models	Resolution	Layers	RCPs
China	BCC-CSM1.1	$1/3^\circ \times 1/3^\circ$	40	2.6, 4.5, 6.0, 8.5
UK	HadGEM2-ES	$1.25^\circ \times 1.875^\circ$	38	2.6, 4.5, 6.0, 8.5
USA	GISS-E2-R	$2^\circ \times 2.5^\circ$	40	2.6, 4.5, 6.0, 8.5

Hydrological models

Three hydrological models are employed to study the uncertainty of model structure in this paper: GR4J, HBV and Xinanjiang. Xinanjiang model with 15 parameters is the most complicated model among the three, and GR4J model with four parameters is the simplest model among the three. The inputs of these models are precipitation and potential evapotranspiration. Potential evapotranspiration is estimated with the Hargreaves equation which uses daily maximum and minimum temperature as inputs (Hargreaves & Samani 1982). These hydrological models are widely used and they were developed based on different

interpretations of the rainfall–runoff processes. The detailed description of the models is listed in the following.

The GR4J model with four parameters is a widely used conceptual model and was developed by the French institute CEMAGREF (Perrin *et al.* 2003). The GR4J model consists of four parameters: the maximum capacity of the production store (X1), the ground water exchange coefficient (X2), the 1 day ahead capacity of the routing store (X3) and the time base of the unit hydrograph (X4). The input of the GR4J model is daily precipitation and potential evapotranspiration, and the output of the model is daily discharge.

The HBV model was developed by the Swedish Meteorological and Hydrological Institute (Bergström 1992). There are eight parameters in the HBV model. The model is composed of a precipitation and snow accumulation routine, a soil moisture routine, a quick runoff routine, a baseflow routine and a transformation function. The inputs of the HBV model are daily precipitation and potential evapotranspiration, and the output is daily discharge. The maximum soil moisture storage (FC) controls the amount of water contributing to the runoff generating routing. The capillary flow from the upper response box to the zone of soil water is described by parameter CFLUX.

The Xinanjiang model was developed by Zhao (1992) for humid and semi-humid regions. There are 15 parameters in the Xinanjiang model. It consists of an evapotranspiration component, a runoff generation component, a runoff production component and a flow routing component. The inputs of the Xinanjiang model are daily precipitation and potential evapotranspiration, and the output is daily discharge.

Calibration and validation of hydrological models

The parameters of GR4J, HBV and Xinanjiang models are calibrated using the historical daily discharges from 1981 to 1990. The validation period is from 1991 to 1995. The uncertainty of parameters in hydrological models has been studied in the previous paper (Xu *et al.* 2013). Therefore, in this paper parameter uncertainty of hydrological models is outside the scope. The Nash–Sutcliffe (NS) efficiency coefficient is used as the objective function in this study. The equation is as follows:

$$\mathrm{NS} = 1 - \frac{\sum_{i=1}^{T} [Q_S(i) - Q_O(i)]^2}{\sum_{i=1}^{T} [Q_O(i) - \bar{Q}_O]^2} \quad (1)$$

where Q_S is the simulated daily discharge (m^3/s), Q_O is the observed daily discharge (m^3/s), i is the number of the days and T is the total number of the days. The maximum value of NS is 1 which means the simulation matches the observation perfectly and the closer to 1 the better it is.

The uncertainties from RCPs, GCMs, downscaling method and hydrologic models are addressed in this study. The extreme high flows are represented by annual maximum daily discharges. To compare the uncertainty range of each source, the uncertainties in simulated high flows from each source are assessed individually in this study. The uncertainty ranges of RCPs are estimated given the average value of design flows for GCMs, hydrologic models and downscaling. In a similar way, the uncertainty ranges are estimated for GCMs, hydrological models and downscaling methods. The design flows with 90% confidence intervals caused by different sources for 10-, 20- and 30-year return periods are estimated to analyze the uncertainty from different sources.

RESULTS

Precipitation and temperature for the baseline and future periods

Figure 2 shows the differences of monthly precipitation between the baseline (1961–1990) and future periods (2011–2040) for four RCPs and three GCMs. It shows that for the same GCM there are different predictions of precipitation in each month under different RCPs. The markers with the largest increase and decrease of monthly precipitation are filled with black in Figure 2.

Uncertainties in precipitation changes due to different GCMs and climate scenarios not only present different magnitudes of changes, but also different directions of change. For BCC-CSM 1.1, there is an increase for most of the time from May to September, and in October there is a decrease. Under RCP2.6, RCP4.5 and RCP6.0, the increase

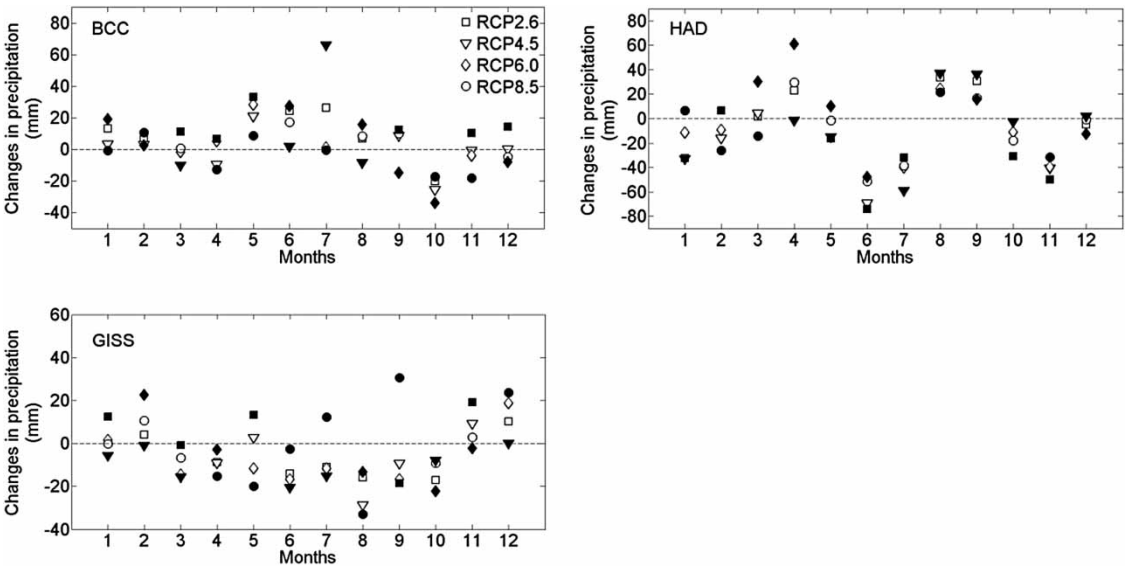

Figure 2 | Changes in monthly mean precipitation between the baseline and future periods.

of annual mean precipitation is 12 mm, 4 mm and 3 mm, respectively. Most of the largest increase for each month is detected under RCP2.6. For HadGEM2-ES, there is a decrease in June, July, October and November and an increase in August and September. Opposite to the annual mean precipitation for BCC-CSM 1.1, the annual mean precipitation decreases under four RCPs and the largest decrease occurs in RCP4.5 with a 13 mm drop. For GISS-E2-R, there is no consistent increase for the four RCPs in each month, and in March, April, August and October the precipitation decreased under all RCPs. The highest increase happens in September under RCP8.5 and for RCP4.5 while the largest decreases occur for 6 months out of a year.

Figure 3 shows the changes of maximum and minimum monthly temperature between the future and baseline periods for three GCMs under four RCPs. The markers with the largest increase and decrease of monthly maximum and minimum temperature are filled with black. Both minimum and maximum temperature increases with different ranges for three GCMs under four RCPs except for the maximum temperature under RCP6.0 for HadGEM2-ES from April to July. For BCC-CSM 1.1 there is the largest increase under RCP8.5 for both maximum temperature and minimum temperature. The increase for the minimum and maximum temperature varies from 0.3 °C to 1.6 °C and 0.1 °C to 1.7 °C respectively. For HadGEM2-ES there is a larger increase for the minimum temperature, which varies from 0.9 °C to 2.6 °C. Under RCP 6.0 the magnitude of increase and decrease for maximum temperature is larger than that under other RCPS. For GISS-E2-R the changes of maximum and minimum temperature are similar. On average there is a larger increase of the minimum temperature compared to the maximum temperature. This is also the case for many areas in the past 50 years (Liu *et al.* 2004; Wang *et al.* 2014). The increase of the temperature is mainly due to the increase of radiative forcing and greenhouse gas concentrations under projected scenarios. In January and February the temperature increases most, which indicates a warmer winter, and there is a smaller increase with fluctuations in other months. It should be noted that RCP8.5 represents a high-end scenario and RCP 2.6 represents a low-end scenario. However, the differences between changes in temperature for different emission scenarios are less obvious in the first half of the 21st century than in the second half of the 21st century, and therefore in the period 2011–2040 the GCM uncertainty is more important. As a result, it is possible that the increase of temperature is the largest for other emission scenarios other than RCP 8.5.

Calibration and validation of hydrologic models

The performance of the three models in the period 1981–1990 is shown in Figure 4. The NS value during the

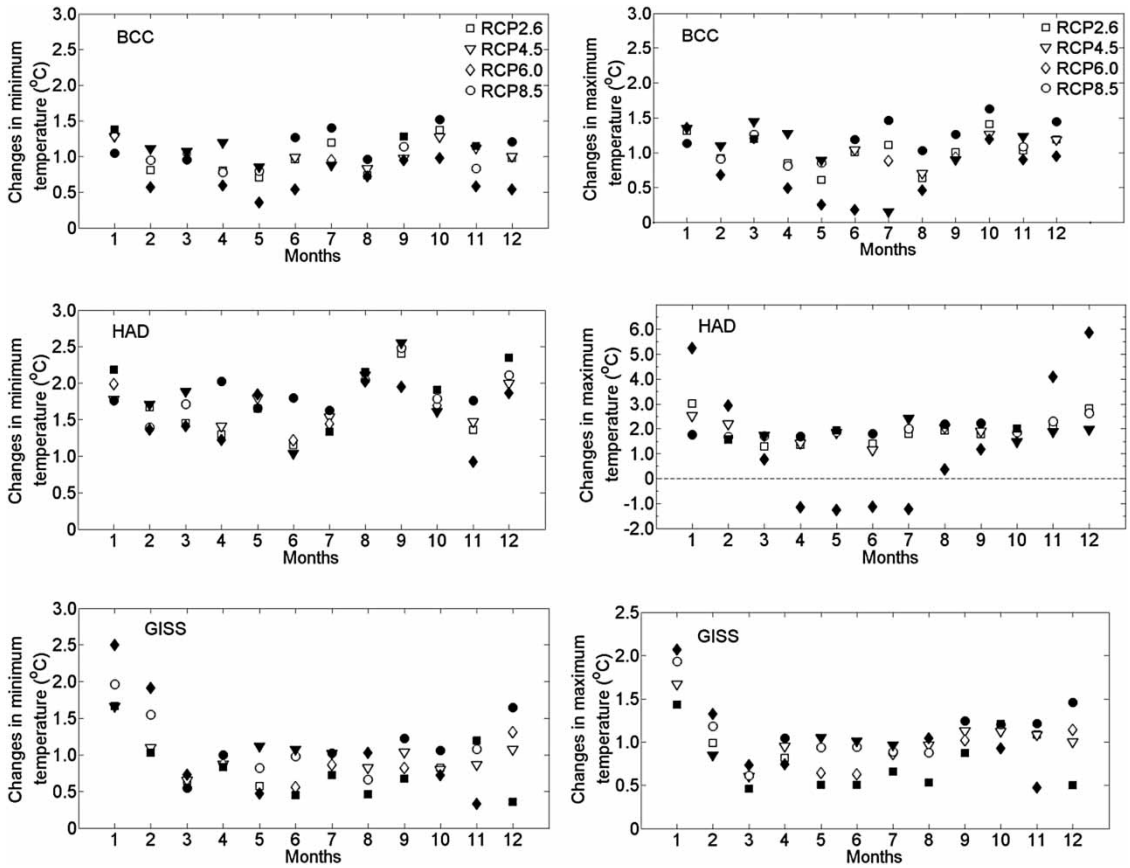

Figure 3 | Changes in minimum (left) and maximum (right) temperature between the baseline and future periods.

calibration and validation for the three models are all above 0.88. The highest NS value in the calibration is 0.91 for the GR4J and HBV model. The three models perform better or equally well in the validation period. The highest NS value is 0.93 for the GR4J model in the validation.

Figure 5 shows the simulation of annual maximum discharges by different models from 1961 to 1990. The annual maximum discharges are fitted by a generalized extreme value (GEV) distribution. For the three models, there are underestimations and overestimations compared to the observed annual maximum discharges. There are more uncertainties in simulation of extreme flows than mean flows because of the relatively limited number of observed extreme flow data (Barsugli *et al.* 2009).

Validation of downscaling method

Before using LARS-WG to generate future climate data, its performance in simulating annual maximum precipitation was checked by the Kolmogorov–Smirnov (K-S) statistical test (Justel *et al.* 1997). The distributions of 30 year observed and 100 year LARS-WG generated annual maximum precipitation in the baseline period is compared (Figure 6). Table 3 shows the L-moment statistics of the compared precipitation, which indicates the good performance of simulating annual maximum precipitation by LARS-WG. $H = 0$ indicates the K-S test cannot reject the null hypothesis that the data follow the same distribution.

Impact of RCPs on the uncertainty ranges of extreme high flows

Figure 7 shows observed extreme high flows in the baseline period and the extreme high flows under the four RCPs in future. The annual maximum discharges are fitted to the GEV distribution and the parameters in the GEV distribution are estimated by the Maximum Likelihood Estimation method. Compared to the baseline period,

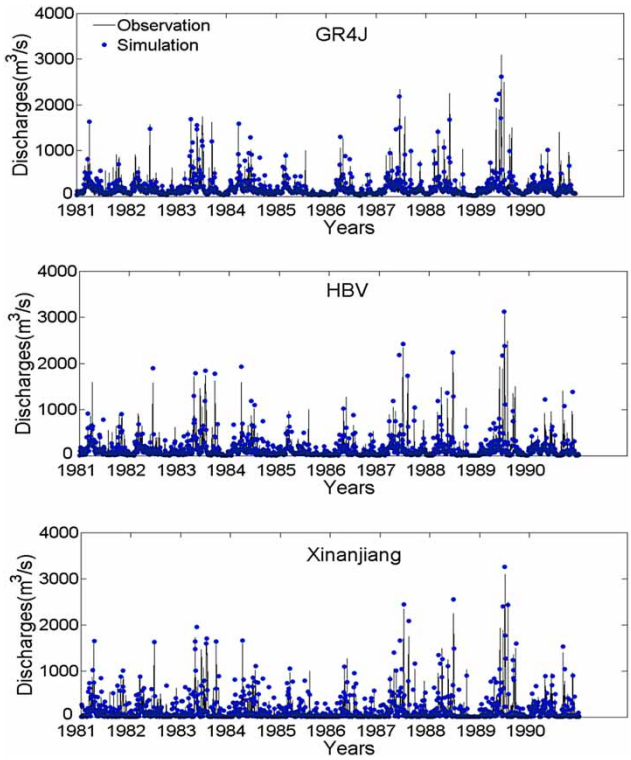

Figure 4 | Performance of three hydrological models for 1981–1990.

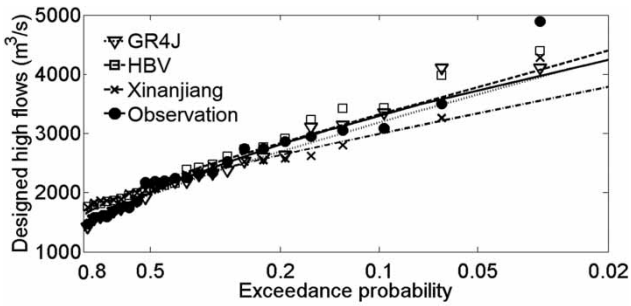

Figure 5 | Comparison of simulated extreme high flows from different models and observations.

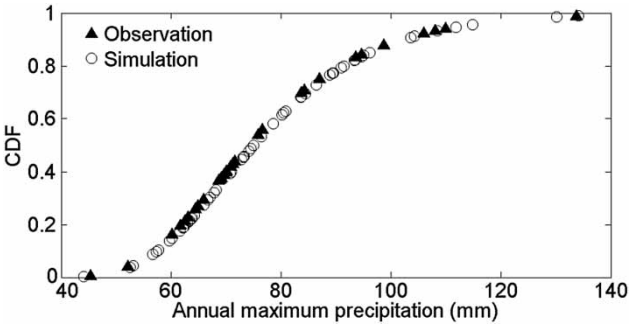

Figure 6 | Empirical cumulative distribution function plots of observed and simulated annual maximum daily precipitation.

Table 3 | L-moment statistic of observed and simulated annual maximum precipitation

	L-mean	L-cv	L-skewness	L-kurtosis	H
Observation	3.72	88.9	4.4	28.9	H = 0
Simulation	3.81	92.7	4.4	28.8	

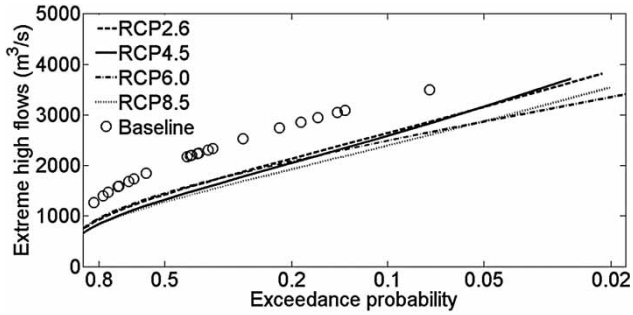

Figure 7 | Exceedance probability of extreme high flows under different RCPs.

there is a decrease for design high flows under four RCPs. The differences of high flows between RCP 2.6, RCP4.5, RCP 6.0 and RCP8.5 are not significant, indicating a small uncertainty range from RCPs.

The degree of uncertainty from other sources under a specific RCP is expressed by a 90% confidence interval, and the 90% confidence intervals for four RCPs are shown in Figure 8. It is shown that although the differences for the average annual maximum discharges from four RCPs are within 100 m^3/s, the uncertainty ranges of annual maximum discharges are 2,000–4,000 m^3/s. The uncertainty ranges with 90% confidence interval under RCP4.5 are larger than those under other climate scenarios with a 10- and 20-year return period. Under RCP8.5 there is a smaller uncertainty range with 90% confidence interval in estimating high flows. Comparing Figures 7 and 8, it should be noted that if considering the uncertainties from GCMs, hydrologic models and downscaling, the directions of future discharge changes are variable and there can be an increase or decrease as shown in Figure 8.

Impact of GCMs on the uncertainty ranges of extreme high flows

Figure 9 shows the extreme high flows for observations in the baseline period and the average extreme high flows for the three GCMs in the future. The future extreme high

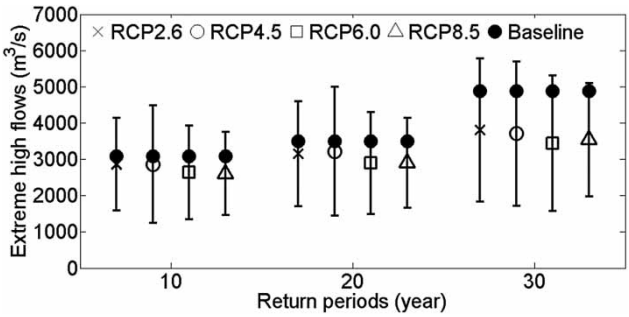

Figure 8 | Extreme high flows with 10-, 20- and 30-year return periods for RCP2.6, RCP4.5, RCP6.0, RCP8.5.

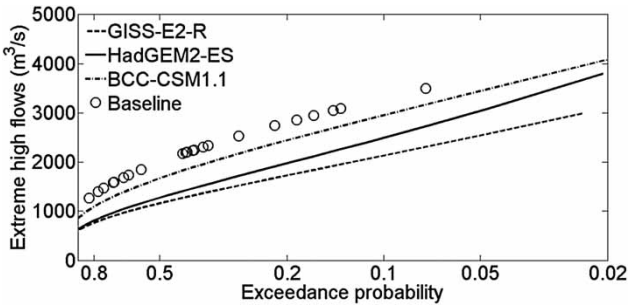

Figure 9 | Exceedance probability of extreme high flows for different GCMs.

flows would decrease for the three GCMs compared to the baseline. Generally, the BCC-CSM 1.1 model simulates larger high flows than HadGEM2-ES and GISS. The GISS model predicts the smallest high flows. The uncertainty range of extreme high flows is the largest for HadGEM2-ES followed by BCC-CSM 1.1, and GISS-E2-R.

Comparing Figures 7 and 9, the uncertainty ranges of extreme high flows for the emission scenarios are smaller than those for the GCMs with corresponding return periods. Considering the other uncertainty sources, i.e. emission scenarios (Figure 10), downscaling method and hydrologic models, for the HadGEM2-ES model the uncertainty range for a 10 year return period is 1,200–4,300 m^3/s and for the GISS model the uncertainty range is 1,400–3,100 m^3/s. For the BCC-CSM 1.1 model the uncertainty range is 2,000–4,200 m^3/s.

Impact of downscaling parameter on the uncertainty ranges of extreme high flows

The outputs from three GCMs are downscaled by LARS-WG. Downscaling is carried out ten times using different random

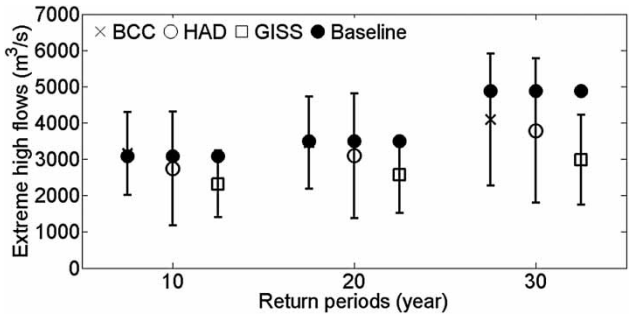

Figure 10 | Extreme high flows with 10-, 20- and 30-year return periods for BCC-CSM 1.1, HadGEM2-ES and GISS-E2-R.

seeds resulting in different meteorological series. Figure 11 shows the differences of average extreme high flows due to different downscaling parameter sets. There would also be a decrease for the extreme high flows for all cases. The uncertainty ranges of extreme high flows due to the downscaling method are smaller than those resulting from GCMs, but larger than those from emission scenarios if compared to Figures 7 and 9. The uncertainty range is 2,400–3,000 m^3/s for a 20-year return period. Previous studies have assessed the ability of LARS-WG in reproducing climate data and its uncertainty by comparing the downscaled monthly mean and variance of temperature and precipitation with observation (Khan *et al.* 2006). This study shows that though there are differences of the annual maximum discharges for choosing different parameter sets in downscaling, the directions of change are consistent.

Impact of hydrologic models on the uncertainty ranges of extreme high flows

Figure 12 shows the extreme high flows for observations in the baseline period and for the three hydrologic models in

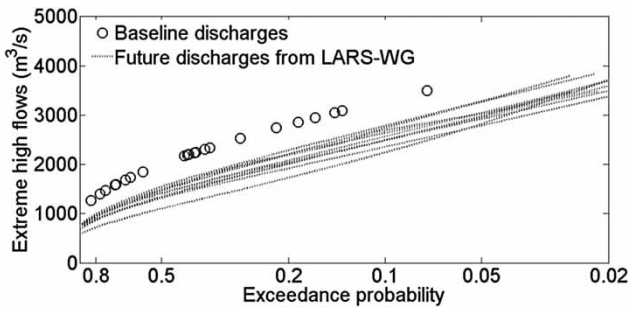

Figure 11 | Exceedance probability of design high flows for downscaling method.

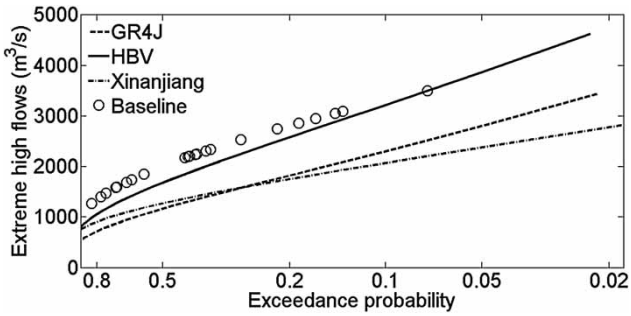

Figure 12 | Exceedance probability of extreme high flows for different hydrologic models.

the future. Except for the results from the HBV model, the extreme high flows estimated by the Xinanjiang model and GR4J model would substantially decrease. Compared with Figures 7, 9 and 11, the uncertainty range of extreme high flows from hydrologic models is larger than from the other uncertainty sources.

Figure 13 shows that the largest uncertainty range of high flows is estimated by the HBV model and the smallest one by the Xinanjiang model. The estimations from the Xinanjiang model and GR4J model show decreases in the future, while the estimations from the HBV model show increases with 100 m^3/s for 10- and 20-year return periods. This is further investigated by comparing the evapotranspiration in the baseline and future period from the three models. The mean increases for the GR4J model and Xinanjiang model range from 1.4 mm to 3.2 mm and 1.3 mm to 3.3 mm respectively. The mean increase of evapotranspiration from the HBV model ranges from 1.2 to 2.4 mm, which is smaller than for the other two models. This could result in a higher simulated discharge than the other two models. Besides, uncertainties related to the model structure

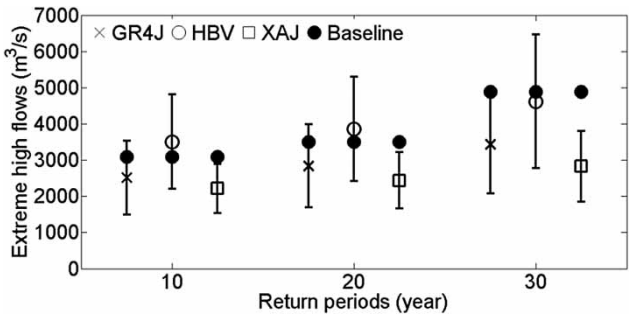

Figure 13 | Extreme high flows with 10-, 20- and 30-year return periods for GR4J, HBV and Xinanjiang.

and parameters could play an important role in the simulation of high flows. In the HBV model, there are separate groups of parameters affecting the high flows series and the total volume balance. For example, a parameter like MAXBAS, which describes the base of the weighting function, is more identifiable during high flow periods and wet seasons and has little effect on the low flow series. Some parameters show a higher identifiability and play a more crucial role in representing the predicted stream flow (Abebe *et al.* 2010). These parameters could affect the simulation of annual maximum discharges in the future differently for the HBV model compared to the Xinanjiang and GR4J models.

DISCUSSION

In this study, four emission scenarios (RCP2.6, RCP4.5, RCP 6.0 and RCP 8.5) were applied to estimate high flows in the near future. The results showed that the uncertainty ranges of high flows from GCMs were larger than those from emission scenarios. Precipitation and temperature were two major inputs to drive the hydrologic models. The average magnitude of the uncertainties of precipitation, maximum and minimum temperature from GCMs and emission scenarios was calculated and compared in Table 4. The bold numbers indicated the larger number between GCMs and emission scenarios. The uncertainties of precipitation, maximum and minimum temperature from the emission scenarios were smaller than those from GCMs in most months, especially for precipitation in spring and summer when heavy rainfall usually occurred and caused floods. These uncertainties in precipitation and maximum and minimum temperature were propagated into the next step of the modeling process, i.e. simulating the discharges. Hence a larger uncertainty of discharges from GCMs was detected than that from emission scenarios.

Model uncertainty was mainly from incomplete and biased knowledge of the rainfall–runoff processes. Studies had been carried out on comparing the uncertainty from different sources in simulating discharges, for instance input error, parameter uncertainty and model structures (Walker *et al.* 2003; Refsgaard *et al.* 2006). Results suggested that there were important benefits in exploring different

Table 4 | Average uncertainty ranges of precipitation, maximum and minimum temperature from GCMs and emission scenarios

Month	Jan	Feb	Mar	Apr	May	Jun	Jul	Aug	Sep	Oct	Nov	Dec
Precipitation(mm)												
RCPs	25	21	**27**	31	27	23	40	20	32	**19**	22	20
GCMs	25	**22**	22	**37**	**38**	**65**	**69**	**51**	**36**	17	**47**	20
Maximum temperature (°C)												
RCPs	1.4	0.7	0.5	**1.3**	**1.4**	**1.5**	1.7	0.9	0.6	0.4	1.0	1.8
GCMs	**1.9**	**1.3**	**0.9**	0.9	1.3	0.9	1.7	**1.2**	**0.8**	**0.7**	**1.7**	**2.3**
Minimum temperature (°C)												
RCPs	0.5	0.6	0.3	0.5	0.4	**0.7**	0.4	0.3	0.5	0.4	**0.7**	0.8
GCMs	**0.9**	**0.9**	**1.0**	**0.7**	**1.0**	0.6	**0.6**	**1.4**	**1.4**	**0.9**	0.6	**1.3**

model structures as part of the overall modeling approach because the model performance was strongly dependent on model structure and different model structures could capture different aspects of the catchment response (Butts *et al.* 2004). In this paper, the GR4J model and Xinanjiang model were more consistent and have a smaller range of uncertainty. The HBV model had the largest uncertainty range and was likely to be more dependent on the input data. Uncertainty ranges of the high flows due to different sources were compared and the results showed that the uncertainty from hydrologic models were the largest compared to GCMs, emission scenarios and the downscaling method, which also confirmed the point that the uncertainty from the hydrological model structure was important and should not be ignored.

In this study, a limited number of GCMs and hydrologic models were applied. It was possible that if more GCMs and hydrologic models were used, the uncertainty ranges from both might change. Besides, it should be noted that the small uncertainty range from emission scenarios was obtained based on the near future period. It was consistent with the fact that the differences of the RCP emission scenarios were small in the beginning and became larger in the second half the 21st century. In Prudhomme's (2003) study, seven GCMs and four scenarios were applied to estimate the floods in UK catchments. Results showed that there was more uncertainty due to the different GCMs than to the emission scenarios, which was in agreement with the result in this paper. In Bae's (2011) study, 13 GCMs, three emission scenarios and three hydrological models were applied to assess water resources in Korea. The results indicated that GCM structures were the main source of uncertainty for summer and autumn in their study area. Although different results could be obtained depending on the methods used and study areas, it should be noted that there were some consistent results stating that the uncertainties from GCMs were large. In this paper, not only the uncertainties from GCMs were noticeable but also the hydrologic models were found with large uncertainties. It was crucial to improve the performance of GCMs and hydrological models to reduce the uncertainty in precipitation and river discharge simulation, particularly high flow simulation, in climate change impact studies.

It was widely acknowledged that the projection of future high flows was important for risk assessment and flood prevention. In this case, the Jinhua River basin was located in the upper reaches of the Qiantang River basin and there was relatively less effect from human activities compared to lower reaches. However, it was also crucial to consider the impact of human activities on the changes of river flows. There were many studies on separating the effects of climate variability and human activities (e.g. Zhang *et al.* 2012, 2013, 2014). The assessment of the contribution of each factor to changes in high flows would be investigated in future study.

In the meantime, considering the large uncertainty existing in climate change impact analysis, quantification of uncertainties from different sources was important to identify the major uncertainty sources and analyze the possible impacts of each uncertainty source on future discharges.

To be supportive for policy makers to make robust and resilient decisions under climate change, it would be more reliable and wholesome if more aspects about uncertainty were involved and we would like to explore it in the next step.

CONCLUSIONS

The uncertainty assessment of high flows due to different uncertainty sources under climate change has been carried out for the Jinhua River basin, eastern China. The climate output from three GCMs under four emission scenarios were downscaled by a statistical downscaling method (LARS-WG) with 10 sets of random seeds. Then, the downscaled outputs were used to drive three lumped hydrologic models. Changes of monthly precipitation, maximum and minimum temperature were compared between the baseline (1961–1990) and future periods (2011–2040). The daily discharges were estimated and extreme high flows represented by T-year flows were calculated for the same periods. The uncertainty ranges of high flows were compared systematically among different sources, including GCMs, RCPs, hydrological models and parameter sets in downscaling.

The results indicated that the uncertainties in precipitation were present in terms of not only the different ranges of changes, but also the directions of change. For the minimum temperature, increases all year round in the future period were found and for the maximum temperature increases were estimated in most cases except for the GISS-E2-R model under RCP 6.0 from April to July. Annual maximum discharges were expected to decrease under four emission scenarios in the near future compared to the baseline period. The magnitudes of decrease of high flows were directly related to the choice of different hydrological models and the RCPs.

Among different uncertainty sources, the analysis showed that hydrologic models and GCMs presented larger uncertainty ranges than parameter sets in downscaling methods and emission scenarios. There was a larger uncertainty range in high flows from the HadGEM2-ES model than that from GISS-E2-R and BCC-CSM 1.1. For hydrologic models, the uncertainty ranges of high flows simulated by the HBV model were larger than those by the GR4J and Xinanjiang models. The changes of average annual maximum discharges were inconsistent, but considering the uncertainty ranges, both the magnitudes and directions of changes would be uncertain. However, the results show that there would be a larger possibility that extreme high flows would decrease, which could indicate a release of pressure on flood prevention. For emission scenarios, RCP8.5 showed the smallest uncertainty compared to other emission scenarios.

ACKNOWLEDGEMENTS

This study was partially supported by the National Natural Science Foundation of China (51379183), Zhejiang Provincial Natural Science Foundation of China (LR14E090001), International Science & Technology Cooperation Program of China (2010DFA24320), Zhejiang Province Postdoc Foundation (BSH1401024) and China Postdoc Foundation (2014M561760). The National Climate Center of China and Bureau of Hydrology, Zhejiang Province are greatly acknowledged for providing weather and flow data in Qiantang River basin.

REFERENCES

Abebe, N. A., Ogden, F. L. & Pradhan, N. R. 2010 Sensitivity and uncertainty analysis of the conceptual HBV rainfall–runoff model: implications for parameter estimation. *J. Hydrol.* **389** (3–4), 301–310.

Alliance, W. U. C. 2009 Options for improving climate modeling to assist water utility planning for climate change. White Paper. www.wucaonline.org/html/ (accessed 22 January 2010).

Bae, D.-H., Jung, I.-W. & Lettenmaier, D. P. 2011 Hydrologic uncertainties in climate change from IPCC AR4 GCM simulations of the Chungju Basin, Korea. *J. Hydrol.* **401** (1–2), 90–105.

Barsugli, J., Anderson, C., Smith, J. B. & Vogel, J. M. 2009 Options for improving climate modeling to assist water utility planning for climate change. www.wucaonline.org/assets/pdf/actions_whitepaper_120909.pdf.

Bell, J. L., Sloan, L. C. & Snyder, M. A. 2004 Regional changes in extreme climatic events: a future climate scenario. *J. Clim.* **17** (1), 81–87.

Bergström, S. 1992 *The HBV model – its structure and applications*. SMHI Reports RH. NO. 4. Norrköping, Sweden.

Butts, M. B., Payne, J. T., Kristensen, M. & Madsen, H. 2004 An evaluation of the impact of model structure on hydrological

modelling uncertainty for streamflow simulation. *J. Hydrol.* **298** (1–4), 242–266.

Calanca, P. & Semenov, M. 2013 Local-scale climate scenarios for impact studies and risk assessments: integration of early 21st century ENSEMBLES projections into the ELPIS database. *Theor. Appl. Climatol.* **113** (3–4), 445–455.

Camici, S., Brocca, L., Melone, F. & Moramarco, T. 2014 Impact of climate change on flood frequency using different climate models and downscaling approaches. *J. Hydrol. Eng.* **19** (8), 04014002.

Chen, J., Brissette, F. P., Chaumont, D. & Braun, M. 2013a Performance and uncertainty evaluation of empirical downscaling methods in quantifying the climate change impacts on hydrology over two North American river basins. *J. Hydrol.* **479**, 200–214.

Chen, X., Yang, T., Wang, X., Xu, C.-Y. & Yu, Z. 2013b Uncertainty intercomparison of different hydrological models in simulating extreme flows. *Water Resour. Manage.* **27** (5), 1393–1409.

Easterling, D. R., Evans, J., Groisman, P. Y., Karl, T., Kunkel, K. E. & Ambenje, P. 2000 Observed variability and trends in extreme climate events: a brief review. *Bull. Am. Meteorol. Soc.* **81** (3), 417–425.

Hargreaves, G. H. & Samani, Z. A. 1982 Estimating potential evapotranspiration. *J. Irrig. Drain. Div.* **108** (3), 225–230.

Hirsch, R. M. 2011 A perspective on nonstationarity and water management. *J. Am. Water Resour. Assoc.* **47** (3), 436–446.

Horton, P., Schaefli, B., Mezghani, A., Hingray, B. & Musy, A. 2006 Assessment of climate-change impacts on alpine discharge regimes with climate model uncertainty. *Hydrol. Process.* **20** (10), 2091–2109.

Houghton, J. T., Callander, B. A. & Varney, S. K. 1992 *Climate change 1992: the supplementary report to the IPCC scientific assessment: [combined with supporting scientific material]*. Cambridge University Press.

Jiang, T., Su, B. & Hartmann, H. 2007 Temporal and spatial trends of precipitation and river flow in the Yangtze River Basin, 1961–2000. *Geomorphology* **85** (3), 143–154.

Jones, C. D., Hughes, J. K., Bellouin, N., Hardiman, S. C., Jones, G. S., Knight, J., Liddicoat, S., O'Connor, F. M., Andres, R. J., Bell, C., Boo, K. O., Bozzo, A., Butchart, N., Cadule, P., Corbin, K. D., Doutriaux-Boucher, M., Friedlingstein, P., Gornall, J., Gray, L., Halloran, P. R., Hurtt, G., Ingram, W. J., Lamarque, J. F., Law, R. M., Meinshausen, M., Osprey, S., Palin, E. J., Parsons Chini, L., Raddatz, T., Sanderson, M. G., Sellar, A. A., Schurer, A., Valdes, P., Wood, N., Woodward, S., Yoshioka, M. & Zerroukat, M. 2011 The HadGEM2-ES implementation of CMIP5 centennial simulations. *Geosci. Model. Dev.* **4** (3), 543–570.

Justel, A., Peña, D. & Zamar, R. 1997 A multivariate Kolmogorov–Smirnov test of goodness of fit. *Stat. Probab. Lett.* **35** (3), 251–259.

Khan, M. S., Coulibaly, P. & Dibike, Y. 2006 Uncertainty analysis of statistical downscaling methods. *J. Hydrol.* **319**, 357–382.

Knox, J. C. 2000 Sensitivity of modern and Holocene floods to climate change. *Quat. Sci. Rev.* **19** (1–5), 439–457.

Knutti, R. & Sedláček, J. 2012 Robustness and uncertainties in the new CMIP5 climate model projections. *Nat. Clim. Chang.* **3**, 369–373.

Kundzewicz, Z., Hirabayashi, Y. & Kanae, S. 2010 River floods in the changing climate – observations and projections. *Water Resour. Manage.* **24** (11), 2633–2646.

Lazzarotto, P., Calanca, P., Semenov, M. & Fuhrer, J. 2010 Transient responses to increasing CO_2 and climate change in an unfertilized grass-clover sward. *Clim. Res.* **41** (3), 221–232.

Liu, B., Xu, M., Henderson, M., Qi, Y. & Li, Y. 2004 Taking China's temperature: daily range, warming trends, and regional variations, 1955–2000. *J. Clim.* **17** (22), 4453–4462.

Lobell, D. B., Burke, M. B., Tebaldi, C., Mastrandrea, M. D., Falcon, W. P. & Naylor, R. L. 2008 Prioritizing climate change adaptation needs for food security in 2030. *Science* **319** (5863), 607–610.

Moss, R. H., Edmonds, J. A., Hibbard, K. A., Manning, M. R., Rose, S. K., van Vuuren, D. P., Carter, T. R., Emori, S., Kainuma, M. & Kram, T. 2010 The next generation of scenarios for climate change research and assessment. *Nature* **463** (7282), 747–756.

Murphy, J. M., Sexton, D. M., Barnett, D. N., Jones, G. S., Webb, M. J., Collins, M. & Stainforth, D. A. 2004 Quantification of modelling uncertainties in a large ensemble of climate change simulations. *Nature* **430** (7001), 768–772.

Nakicenovic, N., Alcamo, J., Davis, G., de Vries, B., Fenhann, J., Gaffin, S., Gregory, K., Grubler, A., Jung, T. Y. & Kram, T. 2000 *Special Report on Emissions Scenarios: A Special Report of Working Group III of the Intergovernmental Panel on Climate Change*. Environmental Molecular Sciences Laboratory, Pacific Northwest National Laboratory, Richland, WA, USA.

Perrin, C., Michel, C. & Andréassian, V. 2003 Improvement of a parsimonious model for streamflow simulation. *J. Hydrol.* **279** (1), 275–289.

Prudhomme, C., Jakob, D. & Svensson, C. 2003 Uncertainty and climate change impact on the flood regime of small UK catchments. *J. Hydrol.* **277** (1–2), 1–23.

Qi, H., Qi, P. & Altinakar, M. S. 2013 GIS-based spatial Monte Carlo analysis for integrated flood management with two dimensional flood simulation. *Water Resour. Manage.* **27** (10), 3631–3645.

Qian, B., Gameda, S. & Hayhoe, H. 2008 Performance of stochastic weather generators LARS-WG and AAFC-WG for reproducing daily extremes of diverse Canadian climates. *Clim. Res.* **37** (1), 17–33.

Refsgaard, J. C., van der Sluijs, J. P., Brown, J. & van der Keur, P. 2006 A framework for dealing with uncertainty due to model structure error. *Adv. Water Resour.* **29** (11), 1586–1597.

Rolf, O. J., Kiang, J. & Waskom, R. 2010 *Workshop on Nonstationarity, Hydrologic Frequency Analysis, and Water Management*. Colorado Water Institute, Colorado, pp. 1–2.

Roshan, G., Ghanghermeh, A., Nasrabadi, T. & Meimandi, J. 2013 Effect of global warming on intensity and frequency curves of precipitation, case study of northwestern Iran. *Water Resour. Manage.* **27** (5), 1563–1579.

Semenov, M. A. 2008 Simulation of extreme weather events by a stochastic weather generator. *Clim. Res.* **35** (3), 203–212.

Semenov, M. A. & Barrow, E. M. 2002 LARS-WG. A stochastic weather generator for use in climate impact studies. User manual. http://www.rothamsted.ac.uk/mas-models/download/LARS-WG-Manual.pdf.

Sena, J., Beser de Deus, L., Freitas, M. & Costa, L. 2012a Extreme events of droughts and floods in Amazonia: 2005 and 2009. *Water Resour. Manage.* **26** (6), 1665–1676.

Sena, J., Freitas, M., de Berrêdo, D. & Fernandes, L. 2012b Evaluation of vulnerability to extreme climatic events in the Brazilian Amazonia: methodological proposal to the Rio Acre basin. *Water Resour. Manage.* **26** (15), 4553–4568.

Shackley, S., Young, P., Parkinson, S. & Wynne, B. 1998 Uncertainty, complexity and concepts of good science in climate change modelling: are GCMs the best tools? *Clim. Change* **38** (2), 159–205.

Tian, Y., Xu, Y.-P., Booij, M. J., Lin, S., Zhang, Q. & Lou, Z. 2012 Detection of trends in precipitation extremes in Zhejiang, east China. *Theor. Appl. Climatol.* **107** (1–2), 201–210.

Tian, Y., Xu, Y.-P. & Zhang, X.-J. 2013 Assessment of climate change impacts on river high flows through comparative use of GR4J, HBV and Xinanjiang models. *Water Resour. Manage.* **27** (8), 2871–2888.

Tian, Y., Booij, M. J. & Xu, Y.-P. 2014 Uncertainty in high and low flows due to model structure and parameter errors. *Stoch. Environ. Res. Risk Assess.* **28**, 319–332.

Tofiq, F. A. & Guven, A. 2014 Prediction of design flood discharge by statistical downscaling and general circulation models. *J. Hydrol.* **517**, 1145–1153.

Van der Keur, P., Henriksen, H. J., Refsgaard, J. C., Brugnach, M., Pahl-Wostl, C., Dewulf, A. & Buiteveld, H. 2008 Identification of major sources of uncertainty in current IWRM practice. Illustrated for the Rhine basin. *Water Resour. Manage.* **22** (11), 1677–1708.

Van Vuuren, D. P., Edmonds, J., Kainuma, M., Riahi, K., Thomson, A., Hibbard, K., Hurtt, G. C., Kram, T., Krey, V. & Lamarque, J.-F. 2011a The representative concentration pathways: an overview. *Clim. Change* **109** (1–2), 5–31.

Van Vuuren, D. P., Edmonds, J. A., Kainuma, M., Riahi, K. & Weyant, J. 2011b A special issue on the RCPs. *Clim. Change* **109** (1), 1–4.

Walker, W. E., Harremoës, P., Rotmans, J., van der Sluijs, J. P., van Asselt, M. B. A., Janssen, P. & Krayer von Krauss, M. P. 2003 Defining uncertainty: a conceptual basis for uncertainty management in model-based decision support. *Integr. Assess.* **4** (1), 5–17.

Wang, F., Zhang, C., Peng, Y. & Zhou, H. 2014 Diurnal temperature range variation and its causes in a semiarid region from 1957 to 2006. *Int. J. Climatol.* **34** (2), 343–354.

Warmink, J. J., Van der Klis, H., Booij, M. J. & Hulscher, S. J. M. H. 2011 Identification and quantification of uncertainties in a hydrodynamic river model using expert opinions. *Water Resour. Manage.* **25** (2), 601–622.

Wilby, R. L. & Harris, I. 2006 A framework for assessing uncertainties in climate change impacts: low-flow scenarios for the River Thames, UK. *Water Resour. Res.* **42** (2), W02419.

Wilby, R. L., Hassan, H. & Hanaki, K. 1998 Statistical downscaling of hydrometeorological variables using general circulation model output. *J. Hydrol.* **205** (1–2), 1–19.

Wu, T. 2012 A mass-flux cumulus parameterization scheme for large-scale models: description and test with observations. *Clim. Dyn.* **38** (3–4), 725–744.

Wu, T., Yu, R. & Zhang, F. 2008 A modified dynamic framework for the atmospheric spectral model and its application. *J. Atmos. Sci.* **65** (7), 2235–2253.

Wu, Z.-Y., Lu, G.-H., Liu, Z.-Y., Wang, J.-X. & Xiao, H. 2013 Trends of extreme flood events in the Pearl River basin during 1951–2010. *Adv. Climate Chang. Res.* **4** (2), 110–116.

Xu, C.-Y., Widén, E. & Halldin, S. 2005 Modelling hydrological consequences of climate change – progress and challenges. *Adv. Atmos. Sci.* **22** (6), 789–797.

Xu, Y.-P., Zhang, X., Ran, Q. & Tian, Y. 2013 Impact of climate change on hydrology of upper reaches of Qiantang River Basin, East China. *J. Hydrol.* **483**, 51–60.

Xu, Y.-P., Zhang, X. & Tian, Y. 2012 Impact of climate change on 24-h design rainfall depth estimation in Qiantang River Basin, East China. *Hydrol. Process.* **26** (26), 4067–4077.

Zakaria, Z., Shabri, A. & Ahmad, U. 2012 Regional frequency analysis of extreme rainfalls in the west coast of peninsular Malaysia using partial L-moments. *Water Resour. Manage.* **26** (15), 4417–4433.

Zhang, A., Zhang, C., Fu, G., Wang, B., Bao, Z. & Zheng, H. 2012 Assessments of impacts of climate change and human activities on runoff with SWAT for the Huifa River basin, northeast China. *Water Resour. Manage.* **26** (8), 2199–2217.

Zhang, C., Shoemaker, C. A., Woodbury, J. D., Cao, M. & Zhu, X. 2013 Impact of human activities on stream flow in the Biliu River basin, China. *Hydrol. Process.* **27** (17), 2509–2523.

Zhang, A., Zhang, C., Chu, J. & Fu, G. 2014 Human-induced runoff change in northeast China. *J. Hydrol. Eng.* **20** (5), 04014069.

Zhao, R. J. 1992 The Xinanjiang model applied in China. *J. Hydrol.* **135** (1–4), 371–381.

First received 14 January 2015; accepted in revised form 3 April 2015. Available online 15 May 2015